AJNR

Myelination in Children with Partial Deletions of Chromosome 18q

Jack L. Lancaster, Jannine D. Cody, Trevor Andrews, L. Jean Hardies, Daniel E. Hale and Peter T. Fox

AJNR Am J Neuroradiol 2005, 26 (3) 447-454
http://www.ajnr.org/content/26/3/447

AJNR Am J Neuroradiol 26:447–454, March 2005

Myelination in Children with Partial Deletions of Chromosome 18q

Jack L. Lancaster, Jannine D. Cody, Trevor Andrews, L. Jean Hardies, Daniel E. Hale, and Peter T. Fox

BACKGROUND AND PURPOSE: **We compared myelin levels in white matter (WM) in typically developing children with those of children with partial deletions of chromosome 18q (18q−).**

METHODS: **Conventional spin-echo MR imaging at 1.9T was used to acquire T1-, T2-, and proton density–weighted images of the brain. From these images, a three-pool model was used to estimate the fraction of water in myelin, myelinated axon, and mixed water compartments (or pools) in six WM regions. A model curve was fit to the pool fractions to model the trend of myelin development by age in each region. Water-pool fractions in children with 18q− aged 5 months to 13 years were compared with those of age-matched, typically developing children.**

RESULTS: **In children with 18q−, the model predicted later onset of myelination ($P < .02$), lower myelination rates ($P < .001$), and smaller equilibrium myelin pool fractions ($P < .001$). Significant differences were seen between the two groups for all three water pool fractions ($P < .001$). The mixed pool fraction was larger in children with 18q−. Although the myelin pool fraction was significantly smaller, the myelinated axon pool fraction was only slightly smaller, leading to a significantly smaller estimate of myelin per myelinated axon in children with 18q− ($P < .001$).**

CONCLUSION: **Myelination modeling in 18q− children indicated delayed onset, a lower rate of myelination, and equilibrium myelin levels less than 50% those of age-matched, typically developing children.**

Children with a deletion of a portion of the long arm of one of the two copies of chromosome 18 (18q) have numerous neurologic deficiencies (1), with a high incidence of dysmyelination of about 95%, as reported from MR imaging studies (2). Children with 18q− can be missing up to 30 Mb of DNA, a region encompassing approximately 100 known genes. All the individuals in our studies with reported dysmyelination were missing a 2-Mb region of 18q23. This region contains seven known genes, one of which encodes for myelin basic protein (MBP) (3). MBP is a key structural protein of myelin in the CNS thought to play a major role in myelin compaction; therefore, it is a logical candidate gene for the dysmyelination phenotype (2, 4), although this has not yet been proved (5, 6). A key diagnostic pattern of dysmyelination in MR imaging is low gray matter (GM)–white matter (WM) contrast on T2-weighted images beyond age 1 year relative to that of healthy children (7–9) (Fig 1). This pattern can persist in individuals with 18q− beyond their first decade. Although low GM-WM contrast may be a diagnostic pattern of delayed or reduced myelin formation, no direct evidence has been reported to confirm this *in vivo*. The purpose of this study was to seek a better understanding of this GM-WM pattern in children with 18q− through modeling of myelin levels during early brain development.

The reductions in GM-WM contrast in the children with 18q− (Fig 1B) versus that of typically developing children (Fig 1A) suggest that this disorder alters T1, T2, and proton density (PD) in WM. MR relaxometry studies have shown that both T1 and T2 relaxation times in WM are significantly longer in children with 18q− than in typically developing children; the change is assumed to be due to dysmyelination (2). Our findings in children with 18q− indicate that proton density is also increased. Although longer relaxation times and increased proton density in WM are consistent with decreased myelin content (10, 11), an

Received January 16, 2004; accepted after revision June 14.

From the Research Imaging Center (J.L.L., T.A., L.J.H., P.T.F.), and Department of Pediatrics (J.D.C., D.E.H.), University of Texas Health Science Center at San Antonio.

Supported by the MacDonald family, Bellevue, WA, and Microsoft Corporation, Redmond, WA.

Address reprint requests to Jack L. Lancaster, PhD, University of Texas Health Science Center at San Antonio, Research Imaging Center, 7703 Floyd Curl Drive, San Antonio, TX 78284.

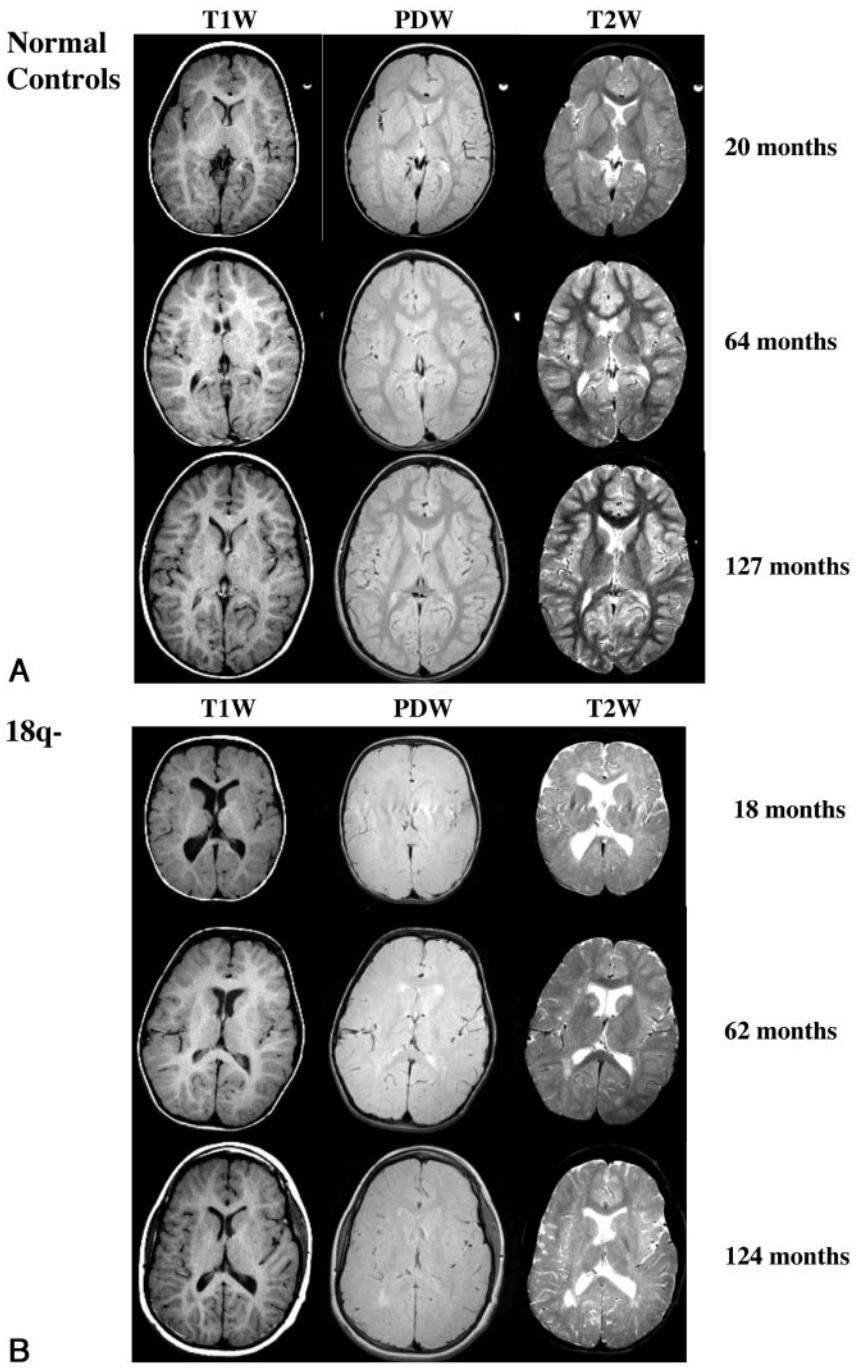

FIG 1. Axial MR images illustrated changes on T1-, PD-, and T2-weighted images with increasing age. *Right* sides of the images represent the right side of the body. Note the inverted T2-weighted contrast at 18 months in the child with 18q− and low T2- and PD-weighted contrast extending to 124 months.

A, Three healthy control children.

B, Three children with 18q−.

appropriate physiological model is needed to test this premise. Models based on MR relaxation characteristics of several water compartments have been used to study the relationship of the myelin compartment to other WM tissue compartments (12–15). However, agreement concerning the number, relaxation characteristics, and biologic meaning of modeled compartments is only moderate.

Increasing evidence suggests that WM can be adequately modeled as three water compartments (14–16). Three water pools have been used to successfully model multiexponential T2 relaxation in frontal WM and optic nerve tissues of bovine brains (16). Three water pools have also been used to characterize MR relaxation properties in human (15) and rat WM tissues (14). Anatomic and physiological changes in WM occurring during myelination provide support for a three-water-pool theory. During myelination in the CNS, glial cells called oligodendrocytes form a multilayer myelin sheath around most axons (17–19). For myelinated axons, the myelin sheath consists of many paired membrane layers. This multimembrane formation becomes a major barrier to water diffusion. Many cells in WM, including unmyelinated axons and glial cells, have a single protein-lipid-protein membrane, and water diffusion through this cell mem-

brane is relatively rapid compared with myelin (20, 21). The multilayered membrane of the myelin sheath effectively forms a water diffusion barrier between myelinated axons and their surrounding environment. This barrier naturally partitions WM into three major distinct water compartments or pools: a myelinated axon pool, a myelin pool, and a mixed pool.

Before myelination, WM consists solely of a mixed pool made up of water in intracellular (unmyelinated axons and glia) and extracellular (interstitial and intravascular) subcompartments (17). Because of the rapid mixing of water within these subpool compartments, the observed relaxation time of the mixed pool is monoexponential, leading to distinct T1 and T2 times. However, during myelination, two new water pools are formed (the myelin pool and the myelinated axon pool), removing unmyelinated axons and myelin-trapped water from the mixed pool. As the water content of the two new pools increases, that of the mixed pool decreases. Importantly, the MR relaxation properties of water in each pool are different due to the different molecular environments of the pools.

For each of the three pools, the within-pool mixing time of water is shorter than the MR relaxation times for mobile water of subpool compartments (15). By following the fast-exchange principle (22), this leads to distinct T1 and T2 relaxation times within each pool. The longest relaxation time is modeled in the mixed pool, intermediate in the myelinated axon pool, and shortest in the myelin pool (15). Because of the slowed diffusion of water molecules by the multimembrane myelin barrier, the between-pool mixing time of water for these three distinct pools is longer than their within-pool mixing times. The interplay of within-pool relaxation times and between-pool mixing times of water determines the net observed relaxation properties in WM (11, 22). These factors result in a single-component exponential T1 relaxation and three-component exponential T2 relaxation in WM, the basis of T1-T2 three-pool modeling in WM (15).

In this study, we estimated the fraction of water in each of the WM water pools in young children by using the three-pool theory. These fractions are assumed to be proportional to the size of corresponding biologic water compartments. For example, the microstructure of each myelin layer is nearly identical, such that with each additional layer of compact myelin additional myelin pool water is accumulated. Similarly, larger diameter myelinated axons are assumed to have a larger myelinated axon water pool. Values for the three pool fractions in typically developing young children were previously reported (15) and were compared with the fractions in children with 18q−. To our knowledge, this is the first report of multicompartmental modeling of WM in a population of children with an assumed dysmyelination condition.

Methods

Subjects

The subjects with 18q− included 13 children (six boys, seven girls) aged 5–161 months (mean ± SD, 69 ± 44 months). Children receiving growth hormone or thyroid hormone treatments were excluded. The control group of typically developing children included 15 children (four boys, 11 girls) aged 3–159 months (mean ± SD, 86 ± 51 months). The healthy and 18q− groups respectively had four and five children younger than 53 months, the time when large changes in myelin occur in the brain (Fig 2). It was extremely hard to recruit these younger children because 18q− is often not detected early enough, and many parents were not willing to travel with such young children to our facility for evaluations. All children with 18q− whose images were analyzed in this study had visual signs of dysmyelination on MR imaging studies (Fig 1B). All imaging was done with the approval of the institutional review board at the University of Texas Health Science Center at San Antonio. Children younger than 5 years were accompanied by a nurse and sedated, if necessary, by using chloral hydrate to ensure minimal movement. If necessary, healthy children younger than 5 years were also sedated, but only with their parents' consent.

MR Imaging Protocol

All images were acquired by using a large-bore 1.9T clinical MR imaging system (Elscint, Haifa, Israel; GE Medical Systems, Milwaukee, WI). Three spin-echo images were acquired: a T1-weighted image (TR/TE, 500/20) and dual-echo PD-weighted/T2-weighted images (TR/TE1/TE2, 3400/20/80), all with NEX = 1. First-order flow compensation was applied before the second echo. Presaturation of a slab inferior to the imaging volume was used to minimize arterial inflow artifacts for all images. Twenty-two axial images were acquired in a 256 × 256 array (1-mm pixel spacing) with 5-mm section thickness and a 1-mm gap (132-mm span). Acquisition time was about 20 minutes, mostly due to the long TR in the dual-echo acquisition. The long TR was used for PD weighting in younger subjects in whom T1 values are longer. Subjects were restrained by using foam pads and Velcro strips to minimize movement between imaging sequences. Children older than 5 years watched their favorite video as a means to reduce motion during imaging. Several imaging studies were incomplete and not analyzed due to motion effects.

T1 relaxation times were calculated by using T1- and PD-weighted images. T1, along with values from the PD-weighted image with T2 relaxation at 20 ms, and the T2-weighted image with T2 relaxation at 80 ms were used with three-pool modeling to estimate the three pool fractions (15).

Regions of Interest and Data Reduction

One author (J.L.L.) manually outlined all regions of interest (ROIs) by using the Alice image processing application (HIPG; Boulder, CO). This was done for consistency in placement, although interrater variability of several of the ROIs was previously shown to be very good (2). ROIs were defined in six prominent WM brain areas including a frontopolar WM area (FWM), an area expected to become myelinated late, and the middle cerebellar peduncle (MCBP), an area expected to become myelinated early. The FWM region contains fibers of the superior longitudinal fasciculus tract, the anterior transverse fasciculus tract, and commissural fibers from the genu of the corpus callosum (CC). A posterior WM region (PWM) region was selected for comparison with the FWM region. The PWM region contains fibers of the superior longitudinal fasciculus tract, the anterior transverse fasciculus tract, and commissural fibers from the splenium of the CC. This region likely included some optical tract fibers. The third large WM region was superior to FWM and PWM regions, above the upper margin of the lateral ventricle, and contains projection fibers from the cortical spinal motor tracts, commissural fibers from the midbody of the CC, and other association fibers. Two distinct regions of the CC were studied: an anterior region (genu) and a posterior region (splenium). Reports have described differ-

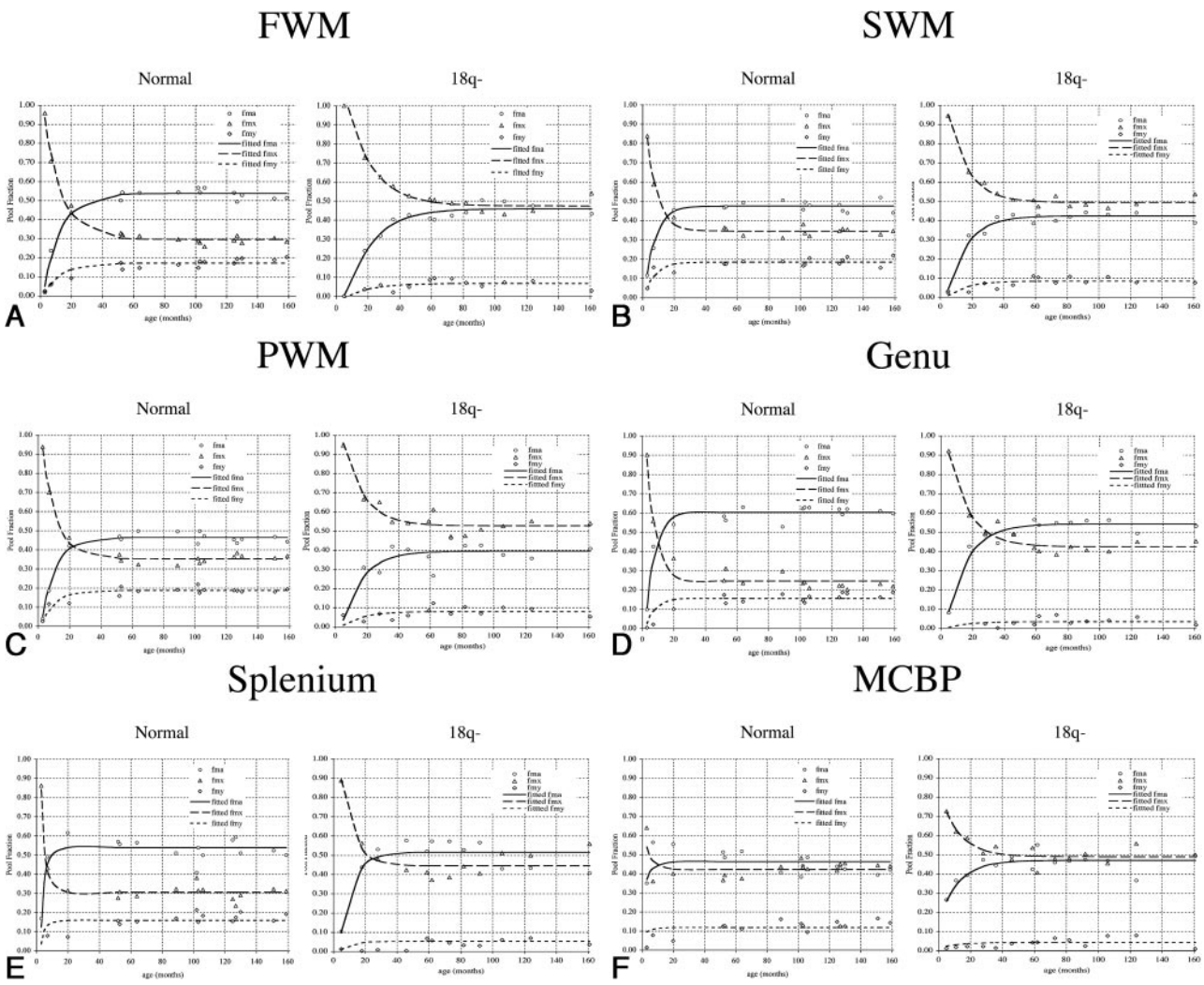

FIG 2. Myelin (f_{my}), myelinated axon (f_{ma}), and mixed (f_{mx}) pool fractions in typically developing children (*normal*) and in children with 18q− as a function of age and the regions in *A–F*.
A, FWM.
B, SWM.
C, PWM.
D, Genu of the CC.
E, Splenium of the CC.
F, MCBP.

ences in timing of myelination for these regions of the CC (9) with the more posterior splenium becoming myelinated earlier.

When we defined ROIs, several strategies were used to minimize partial volume averaging. We traced ROIs well within tissue boundaries and within a single section, while ensuring that the sections above and below had the same WM tissue. The 1-mm gap between sections also served to minimize intersection effects. This ROI placement strategy avoided unwanted signals from the CSF, as others reported (23). ROIs were placed in the left and right hemispheres, and average values calculated. ROIs defined in this manner included data from >100 voxels, which helped to reduce random noise effects. A previous study demonstrated no left-right difference in ROIs (2). The same set of ROIs was used in each of the three MR images (T1, PD, and T2 weighted). All three images were acquired with the same prescribed sections, and co-registration of these images was verified visually. Mathcad (MathSoft, Inc, Cambridge, MA) was used to estimate myelin, myelinated axon, and mixed water pool fractions (f_{my},f_{ma},f_{mx}, respectively) based on average values from the ROIs by using the model Lancaster et al reported (15). Six sets of pool fractions (one set per anatomic region) were calculated for each child. A mathematical model previously applied to study the temporal trend of myelination in healthy children (15) was used to estimate myelination onset time, rate of myelination, and equilibrium water pool fractions for the two groups of children. This modeling was also performed using MathCad (MathSoft, Inc).

Results

Differences between the 18q− and control groups were seen for all three-pool fractions in each of the six regions studied (Fig 2). Differences in the early, rapidly changing phase and the later equilibrium phase of the pool fractions were clearly demonstrated. The myelination model curves fit the trend of measured pool fractions well, with root-mean-square errors of 3.2% ± 1.2% for control subjects and 4.5% ± 0.8% for children with 18q−, averaged over all six ROIs. Group-average values of pool fractions were formally

TABLE 1: Timing parameters from the myelination model

	Onset (months)		TC (months)		Maturation Age (months)	
Region	18q−	Control	18q−	Control	18q−	Control
FWM	6.7 ± 0.54	1.8 ± 1.03	16.3 ± 2.54	10.3 ± 0.30	71.9 ± 10.17	43.2 ± 1.59
SWM	3.6 ± 0.94	0.8 ± 0.16	12.4 ± 0.95	6.3 ± 0.75	53.2 ± 3.93	26.0 ± 3.02
PWM	3.7 ± 1.75	1.9 ± 0.25	12.7 ± 3.59	8.2 ± 0.93	54.5 ± 14.40	34.7 ± 3.74
Genu	2.6 ± 1.10	1.9 ± 0.51	13.1 ± 0.57	5.4 ± 0.27	55.0 ± 2.54	23.5 ± 1.18
Splenium	3.1 ± 0.45	2.3 ± 0.11	8.1 ± 2.44	2.4 ± 0.47	35.5 ± 9.77	11.9 ± 1.90
MCBP	−4.9 ± 0.49	−3.9 ± 0.60	12.1 ± 2.87	4.1 ± 0.47	43.5 ± 11.50	12.5 ± 1.97

Note.—TC is the time constant for myelination model; maturation age, Age when myelin development reaches about 98% of the equilibrium level (onset + 4TC). All SDs estimated by using propagation of errors from Bevington et al (24).

TABLE 2: Pool fractions from the myelination model

	f_{my}		f_{ma}		f_{mx}		f_{my}/f_{ma}	
Region	18q−	Control	18q−	Control	18q−	Control	18q−	Control
FWM	0.067 ± 0.023	0.171 ± 0.021	0.458 ± 0.035	0.536 ± 0.027	0.474 ± 0.036	0.295 ± 0.018	0.147	0.319
SWM	0.085 ± 0.017	0.183 ± 0.021	0.423 ± 0.022	0.475 ± 0.028	0.493 ± 0.027	0.343 ± 0.021	0.200	0.387
PWM	0.079 ± 0.023	0.186 ± 0.012	0.394 ± 0.059	0.463 ± 0.026	0.526 ± 0.045	0.351 ± 0.022	0.200	0.403
Genu	0.034 ± 0.020	0.155 ± 0.020	0.542 ± 0.025	0.602 ± 0.031	0.423 ± 0.026	0.245 ± 0.026	0.063	0.257
Splenium	0.053 ± 0.015	0.157 ± 0.022	0.515 ± 0.075	0.538 ± 0.052	0.444 ± 0.071	0.304 ± 0.038	0.102	0.292
MCBP	0.043 ± 0.025	0.117 ± 0.022	0.469 ± 0.054	0.461 ± 0.041	0.489 ± 0.047	0.421 ± 0.028	0.091	0.254

Note.—f_{my} indicates the myelin pool fraction; f_{ma}, myelinated axon pool fraction; and f_{mx}, mixed pool fraction. Equilibrium fractions are from the model ± SDs of measured fractions about these values for age >4 years.

tested using a two-tailed group *t* test for ages over 80 months where values were similar across age. All three fractions in the 18q− group ($n = 5$) were highly significantly different from those of the control group ($n = 9, P < .001$) in each region. Because children in the two groups could not be paired by age, further group analyses were done by using key parameters from the three-pool myelination model (myelination onset time Δ; myelination time constant TC; and equilibrium pool fractions f_{my}, f_{ma}, and f_{mx}) in each of the six ROIs (Tables 1 and 2).

According to myelination modeling, the onset of myelination was approximately 4–5 months before birth in the MCBP region for both subject groups (Table 1). In all other regions, the onset of myelination was postnatal. The postnatal onset of myelination was later in the 18q− group than in the control group (4.0 ± 1.6 vs. 1.7 ± 0.6 months; paired two-tailed *t* test, $P < .02$). Longer time constants (slower myelination rates) were found in the 18q− group than in control subjects (12.4 ± 2.6 vs. 6.1 ± 2.8 months; paired two-tail *t* test $P < .001$). The largest difference in time constants was seen in the MCBP region, where TC was 4.1 months in control subjects and 12.1 months in the 18q− group. SD estimates for myelination onset time and time constant could not be directly measured; therefore, a propagation-of-errors method was used to estimate SDs for these timing parameters (24).

Consistent with the graphical impression in Figure 2, the model-derived pool fractions for all of the six WM regions were significantly different between the two groups. The myelination model predicted a smaller equilibrium myelin pool fraction (f_{my}, Table 2) in the 18q− group averaged across all regions (6.0% ± 2.0% vs 16.2% ± 2.5%, $P < .0001$). The myelin pool fraction in the control group was more than twice that in the 18q− group in FWM, superior WM (SWM), and PWM regions. This disparity was even greater (about 3 times) for the other WM regions (MCBP, genu, and splenium). The equilibrium myelinated-axon pool fraction (f_{ma}) was also smaller in the 18q− group than in the control group (46.7% ± 5.5% vs. 51.2% ± 5.6%, $P < .01$), but the difference was less than that in the myelin pool. The equilibrium mixed pool fraction (f_{mx}) was significantly larger in the 18q− group than in the control group (47.5% ± 3.7% vs. 32.7% ± 6.0%, $P < .001$). This larger fractional mixed pool water content followed from the constraint that modeled fractions must sum to unity (i.e., if f_{my} and f_{ma} are smaller, f_{mx} is larger). SDs reported in Table 2 were estimated from the scatter of pool fraction data about the model curves for ages >4 years because after this age the model fractions were nearly constant (Fig 2), and most variability was due to data uncertainty. All fractions and their SDs were reported by using three significant figures, (i.e., to 0.1%).

Discussion

Modeling of myelination by age indicated a delay in onset of myelin development and that myelination proceeds at a lower rate in 18q− children than in typically developing children. Although the myelin pool fractions were smaller in the children with 18q−, the myelinated axon pool fractions were only slightly smaller, suggesting that children in the 18q− group form less myelin.

A basic assumption of the three-pool model is that

the three pools are formed when myelin becomes fully compacted (15). Should myelin fail to fully compact, water diffuses more freely among the tissue compartments, and the three-pool model predicts both smaller myelin and myelinated axon water pools. This is an important property of the three-pool model because it does predict diminished myelin functionality for uncompacted myelin.

The three-pool model requires that an increase in the myelin pool fraction (f_{my}) be coupled with a corresponding increase in the myelinated axon pool fraction (f_{ma}), as they are jointly formed. This relationship is seen with increasing age in all cases for the calculated pool fractions (points in Fig 2). The equilibrium f_{my}/f_{ma} relationship is expected to vary in different WM tracts because of differing conduction needs of mature neural circuitry (19). Marked differences in the f_{my}/f_{ma} ratio were seen in the WM regions evaluated (Table 2). The f_{my}/f_{ma} ratio, averaged across all six WM regions, was significantly smaller in the 18q− group (0.131 ± 0.056 vs. 0.319 ± 0.064; group *t* test, $P < .0001$) and approximately 41% that of the control group. If the lower myelin pool fraction (f_{my}) for the 18q− group was due to uncompacted myelin, f_{ma} would also be greatly reduced, and this was not the case (Table 2). Therefore, the decreased myelin-to-myelinated axon ratio in the group with 18q− was most likely due to the large reduction in the myelin pool fraction.

The three-pool myelination model predicted early formation of myelin in the MCBP. This was consistent with findings from previous large-group postmortem (25) and MR imaging studies (26) of brain development. In our control group, the MCBP had the earliest onset time (−3.9 months) and second fastest myelination rate (TC = 4.1 months), indicating early maturation in the MCBP (Fig 2F). This is in contrast to the work by Yakolev and Lacours (25) who the reported onset time of myelination in the MCBP as soon after birth. The prenatal onset times from our myelination model might have been the result of inclusion of WM from the superior and inferior cerebellar peduncles in the ROIs in the younger children, in whom partial volume effects were hard to avoid. This would have introduced error into our measurements because adjacent WM areas are reported to be nearly fully myelinated by birth (26). Our calculations of prenatal onset times for MCBP could also have been related to sampling uncertainty due to the limited number of subjects younger than 2 years. It is also possible that the modeling was correct and that onset time for the MCBP was shortly before birth, but a larger number of younger subjects are needed to clarify this issue.

In our control group, onset of myelination was earliest near the brainstem (4 months before birth in MCBP), at about 1 month in SWM (including motor fibers), and at about 2 months for other regions. The rate of myelination for the FWM region (TC = 10.3 months) was noticeably lower than that of the nearby genu (TC = 5.4 months). To incorporate the effects of both onset time and rate of myelination, we estimated a maturation age for myelin as four time constants (4TC) beyond onset for each of the WM regions (Table 1). The maturation age for FWM in control subjects was predicted to be about 43 months, consistent with other reports (26). The earlier calculated myelination age of the genu relative to the nearby FWM area in both subject groups was consistent with the T2-weighted image contrast between these two areas seen at age 20 months in a healthy child (Fig 1A, top right) and persisting to 62 months in a child with 18q− (Fig 1B, middle right). Although the genu and the splenium of the CC had similar onset times (about 2 months), our modeling indicated that the rate of myelination was higher in the splenium (TC = 2.4 vs. 5.4 months), leading to a maturation age of about 1 year in the splenium and about 2 years in the genu, with an order consistent with other reports (7, 25, 26).

In the children with 18q−, the onset of myelination was also earliest in MCBP (5 months before birth), but their rate of myelination was lower than that of healthy children (TC = 12.1 vs. 4.1 months), leading to a myelin maturation age in this region of approximately 3 years as compared with approximately 1 year in the healthy group. Although the myelin maturation age was always greater in the children with 18q− than in the others, the ranking of maturation age by region was similar in the two groups.

The dysmyelination characteristics of the 18q− group includes delayed onset, a slower rate of progression, and a lower level of myelin at equilibrium. These observations are consistent with the fact that a group of genes on 18q are present in one copy (hemizygous) instead of the usual two copies. In this instance, hemizygosity leads to haploinsufficiency of a rate-limiting component necessary for normal myelin production. Others and we have proposed that this component may be MBP (4, 2); however, this remains to be proved (5, 6). Our modeling clearly indicates decreased levels of myelin (not just altered WM appearance or relaxation times) in children with 18q− that are missing a 2-Mb region of 18q23 inclusive of the MBP gene. Although this is not direct evidence that MBP haploinsufficiency is the cause, our findings help clarify the nature of the WM phenotype. We have evaluated two older individuals with 18q− in their mid 30s, and they also had decreased myelin levels in some brain regions. However, studies of more subjects are needed to confirm that adults with 18q− do not achieve normal levels of myelin.

The smaller myelin pool fraction (f_{my}) in the 18q− group than in the healthy group in all six WM regions indicated that the loss of a region of 18q leads to a global reduction in myelin. In both groups, myelin pool fractions were largest in the FWM, PWM, and SWM regions (17–18% for the control subjects and 7–8% for the 18q− group, for a control-to-18q− ratio of about 2.3:1). These fractions were smallest in the genu, splenium, and MCBP (12–16% for control and 3–5% for 18q−, for a ratio of about 3.5:1). The different control-to-18q− ratio in these two ROI groupings suggests the possibility of a regional myelin

pattern. The pattern of equilibrium myelin fractions (f_{my} in Table 1) for the six regions was compared between the two subject groups, and a large (R = 0.80) marginally significant correlation ($P = .055$, n = 6) was found, suggesting that the pattern relationship between the two groups was probably not a random association. An even higher correlation was seen between the 18q− and control groups for the f_{my}/f_{ma} ratio ($R = 0.95$, $P = .003$). We therefore concluded that the regional myelin pattern in the 18q− group was not significantly different from that in the control group. These analyses provide additional support for a global rather than regional effect of myelin deployment in the 18q− population.

Decreased levels of a required component necessary for normal myelination may lead to altered myelin characteristics with at least two possible outcomes: 1) reduced total myelin of normal structure or 2) similar total myelin of abnormal structure. An autopsy performed on a young female patient with 18q− (2.5 years) reported reduced WM with delayed myelination (27), with no indication of abnormal myelin appearance. Another autopsy performed in an older male patient with 18q− (28 years) revealed that WM in frontal and occipital lobes was reduced, that central WM was well myelinated, and that the CC showed minimal fibrillary gliosis (28). Both patients died from causes not directly related to 18q−. Our modeling, yielding similar myelinated axon pool fractions for both groups (Fig 2, Table 1), strongly suggests that myelin compaction is similar in both groups but with less myelin formed in the 18q− group. To further test for reduced myelin levels in 18q− children, we measured interhemispheric conduction times between the hand motor areas in a small group of typically developing children and in children with 18q− (n = 7 in each group) by using a transcranial magnetic stimulation method (29). The children were aged 70–250 months. These measurements revealed longer interhemispheric conduction times and smaller conduction velocities in the children with 18q−. Conduction velocity increased with age for both groups, indicating a normal trend in myelin production, but the slope of this increase was smaller in the 18q− group than in the control group (0.03 m/s per month vs. 0.05 m/s per month; t test, $P < .001$), consistent with the timing differences for myelin accumulation seen with the three-pool myelination model (Table 1).

A basic assumption of the three-pool model was that T1 and T2 relaxation times could be preassigned for each pool and that the net relaxation times in WM tissues was based on interpool water mixing times (15). Published values for T1 and T2 were assigned to each of the three pools and modified iteratively during calibration. Calibrations were carried out principally in typically developing children such that that the myelin pool fraction in frontal WM was near zero at birth and approached adult levels by age 13 years (15). In Figure 2, most myelin pool fractions were not set equal to zero in this calibration procedure. The present 18q− study used the T1 and T2 values previously determined by using frontal WM ROIs during calibration in typically developing children. The underlying assumption was that the three pools (myelin, myelinated axons, and mixed) had similar intrinsic relaxation properties in both groups of children and that net relaxation differences were due to differences in compact myelin content.

The three-pool model predicts that T1 and T2 values are longest at the onset of myelination (near birth) when most of the water signal intensity arises from the mixed pool because the mixed pool has the longest relaxation time. This is consistent with earlier relaxometry observations (2, 15), with net T1 values in FWM at 3–5 months greater than 2000 ms and net T2 values greater than 100 ms. Both relaxation times shorten as myelination proceeds, and this is believed to be due to the shift of a significant fraction of the water from the mixed pool into the myelin and myelinated axon pools (i.e., those with shorter relaxation times) (Fig 2A).

The changes in contrast observed on T2-weighted MR images during normal brain development (7) are often attributed to a two-compartment model (8); however, our studies with T1 and T2 relaxometry (2, 15) demonstrated the need for an additional pool to adequately model the wide range of age-related changes in T1 and T2 relaxation times. The three-pool model also provides a good explanation for the developmental changes in GM-WM contrast (Fig 2A). The trend of GM-WM contrast in T2-weighted images is that WM is hyperintense at birth (T2 in WM > T2 in GM), and contrast diminishes with age as T2 decreases more rapidly in WM. After the age of approximately 1 year (when T2 of WM becomes shorter than T2 of GM), the WM becomes hypointense (7, 9, 26), matching adult GM-WM contrast. According to the three-pool model, water shifts from the long-relaxation-time mixed pool to the shorter-relaxation-time myelin and myelinated axon pools during myelination (Fig 2), and this change in water pool distribution can lead to the dramatic reduction in the T2 relaxation time of WM relative to GM because of its larger myelin content. This trend was seen in our control group of typically developing children in whom the T2 of FWM was initially longer than the T2 of the caudate (deep GM structure); this reversed by age 20 months (no observations between 7 and 20 months), maintaining an adult GM-WM contrast pattern through the upper age range studied (about 13 years). Although the caudate had a higher density of myelinated axons than cortical GM, it was selected for this analysis because cortical GM could not be accurately delineated in younger children.

Conclusion

The temporal pattern of myelination predicted by using three-pool modeling in a small group of typically developing children was consistent with that reported in other large-group studies. Modeling of

myelin water indicated that children with 18q deletions, encompassing a 2-Mb region of 18q23, produce less myelin than typically developing children, although they have similar modeled values for myelinated axons. The dysmyelination pattern appears to be global, with all brain regions tested having less than 50% the myelin water pool levels of healthy children. Delayed onset and a decreased rate of myelination were also seen in the children with 18q−.

References

1. Kline AD, White ME, Wapner R, et al. **Molecular analysis of the 18q- syndrome: and correlation with phenotype.** *Am J Hum Genet* 1993;52:895–906
2. Gay CT, Hardies LJ, Rauch RA, Lancaster, et al. **Magnetic resonance imaging demonstrates incomplete myelination in 18q- syndrome: evidence for myelin basic protein haploinsufficiency.** *Am J Med Genet* 1997;74:422–431
3. Kamholz j, Spielman R, Gogolin K, Modi W, O'Brien S, Lazzarini R. **The human myelin-basic-protein gene: Chromosomal localization and RFLP analysis.** *Am J Hum Genet* 1987;40:365–373
4. Loevner LA, Shapiro RM, Grossman RI, Overhauser J, Kamholz J. **White matter changes associated with the deletions of the long arm of chromosome 18 (18q- syndrome): a dysmyelinating disorder?** *AJNR Am J Neuroradiol* 1996;17:1843–1848
5. Gabrielli O, Coppa GV, Carloni I, Salvolini U. **18q- syndrome and white matter alterations [comment].** *AJNR Am J Neuroradiol* 1998;19:398
6. Barker LE. **18q- syndrome and white matter alterations [comment].** *AJNR Am J Neuroradiol* 1998;19:399
7. Barkovich AJ, Kjos BO, Jackson DE, Normal D. **Normal maturation of the neonatal and infant brain: MR imaging at 1.5T.** *Neuroradiology* 1988;166:173–180
8. Barkovich AJ. **Concepts of myelin and myelination in neuroradiology.** *AJNR Am J Neuroradiol* 2000;21:1099–1109
9. Dietrich RB. **Maturation, myelination, and dysmyelination.** In: Stark DD, Bradley WG, eds. *Magnetic Resonance Imaging*, 3rd ed. Vol 3. St Louis:Mosby–Year Book; 1999:1425–1447
10. Koenig SH, Brown RD, Spiller M, Lundbom N. **Relaxometry of brain: Why white matter appears bright in MRI.** *Magn Reson Med* 1990;14:482–495
11. Fischer HW, Rinck PA, Haverbeke YV, Muller RN. **Nuclear relaxation of human brain gray and white matter: analysis of field dependence and implications in MRI.** *Magn Reson Med* 1990;16:317–334
12. Whiteall KP, MacKay AL, Graeb DA, Nugent RA, Li DKB, Paty DW. **In vivo measurement of T2 distributions and water contents in normal human brain.** *Magn Reson Med* 1997;37:34–43
13. Stanisz GJ, Kecojevic A, Bronskill MJ, Henkelman RM. **Characterizing white matter with magnetization transfer and T2.** *Magn Reson Med* 1999;42:1128–1136
14. Does MD, Gore JC. **Compartmental study of T1 and T2 in rat brain and trigeminal nerve in vivo.** *Magn Reson Med* 2002;47:274–283
15. Lancaster JL, Andrews TA, Hardies LJ, Dodd S, Fox PT. **Three-pool model of white matter.** *J Magn Reson Imaging* 2003;17:1–10
16. Andrews T, Lancaster JL, Dodd SJ, Contreras-Sesvold V, Fox PT. **Testing the three-pool model adapted for use with T2 relaxometry.** *Magn Reson Med* 2004. In press.
17. Davison AN, Peters A. **Myelination**. Springfield: Charles C. Thomas; 1970
18. Morell P, Quarles RH, Norton WT. **Myelin formation, structure, and biochemistry.** In: Siegel JS, Agranoff BW, Albers RW, Molinoff PB, eds. *Basic Neurochemistry: Molecular, Cellular, and Medical Aspects*. 5th ed. New York: Raven; 1993:117–144
19. Hirano A, Llena JF. **Morphology of central nervous system axons.** In: Waxman SG, Kocsis JD, Stys PK, eds. *The Axon: Structure, Function and Pathophysiology*. New York: Oxford University Press; 1995:49–67
20. Guyten AC. *Textbook of Medical Physiology.* 4th ed. Philadelphia: W. B. Saunders; 1971:39–51
21. Finkelstein A. *Water Movement through Lipid Bilayers, Pores, and Plasma Membrane: Theory and Reality.* New York: Wiley-Interscience; 1987:153–184
22. Zimmerman JR, Brittin WE. **Nuclear magnetic resonance studies in multiple phase systems: lifetime of a water molecule in an adsorbing phase on silica gel.** *Phys Chem* 1957;6:1328–1333
23. MacKay A, Whittall K, Adler J, Li D, Paty D, Graeb D. **In vivo visualization of myelin water in brain by magnetic resonance.** *Magn Reson Med* 1994;31:673–677
24. Bevington PR, Robinson DK. **Data reduction and error analysis for the physical sciences.** 2nd ed. New York: Mc-Graw-Hill; 1992
25. Yakovlev PI, Lecours AR. **The myelogenetic cycles of regional maturation of the brain.** In: Minkowski A, ed. *Regional Development of the Brain in Early Life.* Oxford: Blackwell; 1967:539
26. Ballesteros MC, Hansen PE, Soila K. **MRI imaging of the developing human brain, II: postnatal development.** *Radiographics* 1993;13:611–622
27. Felding I, Kristoffersson U, Sjostrom H, Noren O. **Contribution to the 18q- syndrome. A patient with del (18)(q22.3qter).** *Clin Genet* 1987;31:206–210
28. Vogel H, Urich H, Horoupian DS, Wertelecki W. **The brain in the 18q- syndrome.** *Dev Med Child Neurol* 1990;32:725–742
29. Meyer BU, Roricht S, von Einsiedel HG, Kruggel F, Weindl A. **Inhibitory and excitatory interhemispheric transfers between motor cortical areas in normal humans and patients with abnormalities of the corpus callosum.** *Brain* 1995;118:429–440